



## Oxidative stress and histopathological alterations in the lungs and brains of Wistar rats following single and combined exposure to Dichlorvos, Dimethoate and Cypermethrin

Adeyemi Oyeyemi<sup>1\*</sup>, Sunday Ogheneruemu Samson<sup>2</sup>

<sup>1</sup> Department of Environmental Management, Toxicology & Biochemistry, Federal University of Petroleum Resources, Effurun, Nigeria

<sup>2</sup> Department of Environmental Management and Toxicology, Federal University of Petroleum Resources, Effurun, Nigeria

### Abstract

This study evaluated oxidative stress responses in the lungs and brains of Wistar albino rats exposed to dichlorvos, dimethoate, cypermethrin, and their combinations. Antioxidant enzyme activities and malondialdehyde (MDA) levels were quantified, while histopathological alterations were assessed to establish mechanistic insights. Results showed a significant stepwise induction of superoxide dismutase (SOD) in both lungs and brain across exposure groups ( $p < 0.05$ ). The highest activities were observed in the triple-insecticide group (H), with lung SOD reaching 0.0056 U/mg protein and brain SOD peaking at a similar magnitude, significantly surpassing controls. Catalase activity followed a comparable trend. In the lungs, Groups A and B showed the lowest values, whereas Group H displayed the maximum induction (0.1819 U/mg protein), representing a robust adaptive response. The brain exhibited sharper distinctions, with Groups F and H showing significant elevations, indicating heightened neuronal susceptibility. Lipid peroxidation, measured as MDA, increased markedly across treatments. Lung MDA rose from 0.00071 nmol/mg protein in controls to 0.00171 nmol/mg protein in Group H, while brain MDA peaked at 0.0013 nmol/mg protein, demonstrating cumulative oxidative injury. Histopathology confirmed these biochemical findings: lungs showed alveolar collapse, bronchiolar necrosis, and vascular degeneration, while brains displayed neuronal pyknosis, axonal degeneration, and clumping. In conclusion, both lungs and brains exhibited significant oxidative stress under pesticide exposure, with the triple-insecticide combination eliciting the most severe biochemical and structural damage. These findings underscore the synergistic toxicity of pesticide mixtures and highlight SOD, catalase, and MDA as reliable biomarkers of pulmonary and neural oxidative stress.

**Keywords:** Oxidative stress, pesticide mixtures, superoxide dismutase, malondialdehyde, histopathology

### Introduction

The extensive use of synthetic pesticides has become an integral component of modern agricultural practices and domestic pest control, particularly in developing countries where regulatory enforcement is often weak and public awareness of toxicological risks remains limited (He *et al.*, 2022) <sup>[17]</sup>. Among these chemical agents, organophosphate and pyrethroid insecticides are widely favoured due to their broad-spectrum efficacy, rapid action, and perceived safety when used at recommended doses (Lucero & Muñoz-Quezada, 2021). Dichlorvos and dimethoate, both organophosphate compounds, and cypermethrin, a synthetic pyrethroid, are among the most commonly applied insecticides in agricultural fields, storage facilities, and residential environments (Shaikh & Rs, 2020) <sup>[45]</sup>. However, increasing experimental and epidemiological evidence suggests that repeated or combined exposure to these compounds may pose significant risks to non-target organisms, including humans and wildlife, through mechanisms that extend beyond their intended neurotoxic effects on insects (Bradford *et al.*, 2020).

Pesticide exposure in real-world settings rarely occurs in isolation. Farmers, applicators, and the general population are often simultaneously or sequentially exposed to multiple pesticide formulations through inhalation, ingestion of contaminated food and water, and dermal contact (Craig *et al.*, 2020) <sup>[9]</sup>. Such mixed exposures are of particular concern because chemical interactions between compounds may result in additive, synergistic, or potentiated toxic effects that are not predictable from single-compound

assessments (Kassotis & Phillips, 2023). Regulatory toxicology has traditionally focused on evaluating individual active ingredients, thereby underestimating the health risks associated with pesticide mixtures. Consequently, there is a growing need for experimental studies that examine the combined toxicological impacts of commonly co-used insecticides on vital organs and biological systems.

Oxidative stress has emerged as a central mechanism underlying pesticide-induced toxicity in mammalian systems (Sevim *et al.*, 2021) <sup>[44]</sup>. It is characterised by an imbalance between the production of reactive oxygen species and the capacity of endogenous antioxidant defences to neutralise them. Excessive reactive oxygen species can attack cellular lipids, proteins, and nucleic acids, leading to structural damage, impaired cellular signalling, and eventual cell death (Jomová *et al.*, 2023) <sup>[20]</sup>. Organophosphate and pyrethroid insecticides have been shown to enhance reactive oxygen species generation through metabolic activation and disruption of mitochondrial function, making oxidative stress a unifying pathway through which pesticides exert toxic effects across multiple organs (Farkhondeh *et al.*, 2020) <sup>[11]</sup>.

The lungs represent a critical portal of entry for airborne pesticide particles and vapours, particularly during spraying and fumigation activities. Inhalational exposure allows these compounds to bypass first-pass hepatic metabolism, leading to direct interaction with pulmonary tissues (Langenbach *et al.*, 2021) <sup>[25]</sup>. The lung's extensive surface area, rich vascularisation, and high oxygen tension make it especially

vulnerable to oxidative injury. Oxidative stress in pulmonary tissue can compromise alveolar integrity, disrupt gas exchange, and initiate inflammatory cascades that predispose to chronic respiratory dysfunction (Bezerra *et al.*, 2023) [6]. Despite this vulnerability, the lungs have received comparatively less attention in pesticide toxicology studies than the liver and kidney, creating a significant gap in understanding respiratory outcomes.

Similarly, the brain is highly susceptible to oxidative damage due to its elevated oxygen consumption, abundance of polyunsaturated fatty acids, and relatively limited antioxidant capacity (Rodrigues *et al.*, 2022) [38]. Although the blood–brain barrier provides partial protection, many pesticides are sufficiently lipophilic to cross this barrier and accumulate in neural tissues. Beyond classical mechanisms such as acetylcholinesterase inhibition by organophosphates and sodium channel modulation by pyrethroids, oxidative stress has been increasingly implicated in pesticide-induced neurotoxicity, contributing to neuronal degeneration and synaptic dysfunction (Farkhondeh *et al.*, 2020) [11].

Antioxidant enzymes constitute a major line of defence against oxidative injury. Superoxide dismutase catalyses the conversion of superoxide radicals into hydrogen peroxide, while catalase decomposes hydrogen peroxide into water and molecular oxygen, preventing the formation of highly reactive hydroxyl radicals (Anwar *et al.*, 2024) [3]. Alterations in the activities of these enzymes reflect the cellular response to oxidative challenges and provide insight into the severity of toxic insults. Concurrently, lipid peroxidation products such as malondialdehyde serve as reliable indicators of oxidative damage to cellular membranes (Gaschler & Stockwell, 2017) [14].

Histopathological evaluation complements biochemical assessments by revealing structural and cellular alterations induced by toxic exposure. Changes such as tissue necrosis, inflammatory infiltration, and architectural distortion provide tangible evidence of organ damage and allow correlation with biochemical markers of oxidative stress (Banerjee *et al.*, 2023) [4]. In the lungs, pesticide-induced injury may manifest as alveolar collapse and bronchiolar degeneration, while in the brain, neuronal degeneration and glial alterations may occur. Together, biochemical and histological analyses provide a comprehensive framework for understanding pesticide toxicity (Elmorsy *et al.*, 2022) [10].

Animal models, particularly Wistar albino rats, remain indispensable tools for elucidating the systemic effects of toxicants under controlled experimental conditions (Massoud *et al.*, 2022) [29]. Their physiological similarities to humans make them suitable for investigating organ-specific toxicity and mechanistic pathways, including the evaluation of combined pesticide exposures and potential synergistic interactions.

Given the widespread and overlapping use of dichlorvos, dimethoate, and cypermethrin in agricultural and domestic settings, it is imperative to evaluate their combined toxicological effects on organs highly sensitive to oxidative injury (Serdar *et al.*, 2023) [42]. Understanding how these compounds interact to influence antioxidant defence systems and tissue integrity is crucial for improving risk-assessment frameworks and informing regulatory policies, particularly in regions where pesticide misuse and

environmental contamination are prevalent (Okonkwo *et al.*, 2023) [34].

Therefore, the present study was designed to investigate oxidative stress responses and histopathological alterations in the lungs and brains of Wistar albino rats exposed to dichlorvos, dimethoate, cypermethrin, and their combinations. By integrating antioxidant enzyme assays, lipid peroxidation analysis, and detailed tissue histopathology, this study provides mechanistic insight into organ-specific and combined insecticide toxicity and underscores the importance of considering mixture effects in toxicological evaluation and public health decision-making.

## Materials and Methods

### Animals

Twenty-four healthy postpartum female Wistar albino rats (*Rattus norvegicus*), weighing 180–200 g, were obtained from the Animal House, Department of Environmental Management and Toxicology, Federal University of Petroleum Resources, Effurun, Nigeria. The animals were housed in standard cages under controlled laboratory conditions (temperature  $23 \pm 2$  °C; relative humidity 50–60%; 12 h light/12 h dark cycle). Rats had free access to commercial pelleted feed and clean tap water throughout the experimental period. All procedures were conducted in accordance with institutional ethical guidelines for animal experimentation and were approved by the University Ethical Review Committee (Approval No.: EMT/2025/012).

### Chemicals

Technical-grade dichlorvos (98%), dimethoate (97%), and cypermethrin (95%) were purchased from Sigma-Aldrich (USA). Stock solutions were prepared using distilled water. All other reagents used for biochemical analyses were of analytical grade.

### Experimental Design and Treatment Protocol

Postpartum female Wistar albino rats were randomly assigned into eight experimental groups ( $n = 4$  per group): Group A (control, water spray), Group B (dichlorvos), Group C (dimethoate), Group D (cypermethrin), Group E (dichlorvos + dimethoate), Group F (dichlorvos + cypermethrin), Group G (dimethoate + cypermethrin), and Group H (dichlorvos + dimethoate + cypermethrin).

Insecticide solutions were freshly prepared at a concentration of 1.33 mL/L and administered by spraying at a dose rate of 0.05 mL/m<sup>2</sup> to simulate environmental exposure conditions. Treatments were applied once daily for 28 consecutive days. At the end of the exposure period, animals were anaesthetised using light ether vapour and humanely sacrificed. Blood samples were collected by cardiac puncture, and brain and lung tissues were excised immediately, rinsed in ice-cold normal saline, and processed for biochemical and histopathological analyses.

### Tissue Preparation

Brain and lung tissues were rinsed in ice-cold saline, blotted dry, and homogenised to obtain 10% (w/v) homogenates in 0.1 M phosphate buffer (pH 7.4). Homogenates were centrifuged at  $10,000 \times g$  for 15 min at 4 °C, and the supernatants were collected and stored at –8 °C until biochemical assays.

## Biochemical Assays

### Superoxide Dismutase (SOD) Activity:

SOD activity was determined using the adrenaline auto-oxidation method, which is based on the enzyme's ability to inhibit the oxidation of adrenaline to adrenochrome in an alkaline medium. The rate of adrenochrome formation was monitored spectrophotometrically at 480 nm, and SOD activity was expressed as units per milligram protein (Misra & Fridovich, 1972)<sup>[31]</sup>.

### Catalase (CAT) Activity

Catalase activity was assayed by measuring the decomposition of hydrogen peroxide. Residual hydrogen peroxide reacts with potassium dichromate in acetic acid upon heating to form chromic acetate, the intensity of which was measured at 570 nm. Catalase activity was expressed as units per milligram protein following the method described by Sinha (1972)<sup>[46]</sup>.

### Malondialdehyde (MDA) Concentration

Lipid peroxidation was assessed by estimating malondialdehyde levels using the thiobarbituric acid reactive substances (TBARS) assay. Under acidic conditions and elevated temperature, MDA reacts with thiobarbituric acid to form a coloured adduct, which was measured spectrophotometrically at 535 nm. Results were expressed as nmol MDA per milligram protein (Ohkawa, Ohishi, & Yagi, 1979)<sup>[33]</sup>.

### Histopathological Examination

Portions of brain and lung tissues were fixed in 10% neutral buffered formalin for 48 h, dehydrated in ascending grades of ethanol, cleared in xylene, and embedded in paraffin wax. Sections of 5  $\mu$ m thickness were cut, mounted on glass slides, and stained with haematoxylin and eosin (H&E). Slides were examined under a light microscope (Olympus CX43, Japan), and representative photomicrographs were captured.

## Statistical Analysis

All data were expressed as mean  $\pm$  standard error of the mean (SEM) ( $n = 4$ ). Statistical analysis was performed using one-way analysis of variance (ANOVA), followed by Tukey's post hoc test. Statistical significance was accepted at  $p < 0.05$ . Analyses were conducted using SPSS version 25.0 (IBM Corp., Armonk, NY, USA).

## Results

As shown in Figure 1a, lung superoxide dismutase (SOD) activity did not differ significantly between Groups A and B ( $p > 0.05$ ), and both groups exhibited the lowest enzyme activities. A significant elevation was observed in Group C relative to Groups A and B ( $p < 0.05$ ). Groups D and E showed comparable activities ( $p > 0.05$ ), although both were significantly higher than those recorded in the preceding groups. Similarly, Groups F and G did not differ significantly from each other ( $p > 0.05$ ) but demonstrated significantly greater SOD activities than Groups D and E ( $p < 0.05$ ). The highest lung SOD activity was recorded in Group H, which was significantly greater than all other groups ( $p < 0.05$ ). Overall, these results indicate a progressive induction of lung SOD activity following insecticide exposure, with combined treatments eliciting the most pronounced response.

A comparable pattern was observed for brain SOD activity in Figure 1b. Groups A and B exhibited similarly low activities, with no significant difference between them ( $p > 0.05$ ). Groups C and D showed significant increases relative to Groups A and B ( $p < 0.05$ ), although their values were statistically comparable. Groups E and F also displayed similar activities ( $p > 0.05$ ), both of which were significantly higher than those observed in Groups A–D ( $p < 0.05$ ). A further significant elevation was evident in Group G ( $p < 0.05$ ), while the greatest brain SOD activity was recorded in Group H, which differed significantly from all other groups ( $p < 0.05$ ).

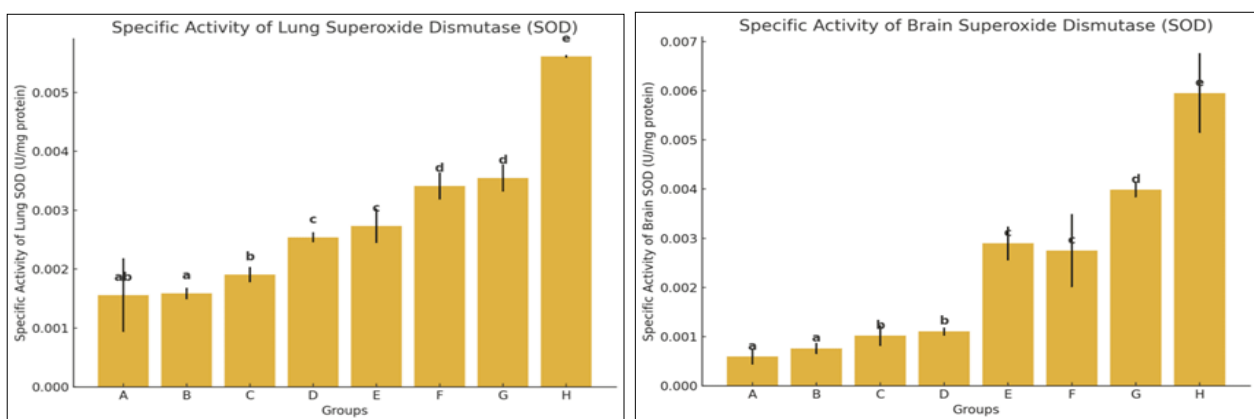


**Fig 1:** Specific Activity of Lung and Brain Superoxide Dismutase (SOD) in Rats Exposed to Dichlorvos, Dimethoate, and Cypermethrin Singly and in Combination. Plotted values are means  $\pm$  SEM. Bars carrying different alphabetical notations are significantly different ( $p < 0.05$ )

As presented in Figure 2a, lung catalase activity did not differ significantly between Groups A and B ( $p > 0.05$ ), with both groups exhibiting the lowest enzyme activities. A significant increase was observed in Group C relative to Groups A and B ( $p < 0.05$ ). Group D occupied an intermediate position, showing no significant difference when compared with either Group B or Group C ( $p > 0.05$ ). Groups E and F demonstrated comparable catalase activities

( $p > 0.05$ ) and were significantly higher than those of Groups A and B ( $p < 0.05$ ), although their values were not markedly different from those of Groups C and D. Group G clustered with the intermediate-response groups, showing no significant difference relative to them ( $p > 0.05$ ). In contrast, Group H exhibited the highest liver catalase activity, which was significantly greater than that of all other groups ( $p < 0.05$ ). Collectively, these findings indicate a progressive

induction of liver catalase activity with increasing insecticide exposure, with the most pronounced response occurring in the triple-insecticide treatment. Figure 2b illustrates the pattern of brain catalase activity, which differed slightly from that observed in the liver. Group A recorded the lowest activity and was significantly lower than all other groups ( $p < 0.05$ ). Group B showed a significant elevation compared with Group A ( $p < 0.05$ ), whereas Group C did not differ significantly from either Group B or Group D ( $p > 0.05$ ), indicating an overlap among these groups.

Although Group D displayed higher activity than Group A, its catalase level remained relatively modest and was statistically comparable to that of Group C. A marked increase was evident in Group E, which was significantly higher than Groups A–D ( $p < 0.05$ ). Group F exhibited a further significant elevation, surpassing Groups A–E ( $p < 0.05$ ). Group G did not differ significantly from Groups E or F ( $p > 0.05$ ), suggesting a shared response range among these treatments. The highest brain catalase activity was recorded in Group H, which was significantly greater than all other groups ( $p < 0.05$ ).

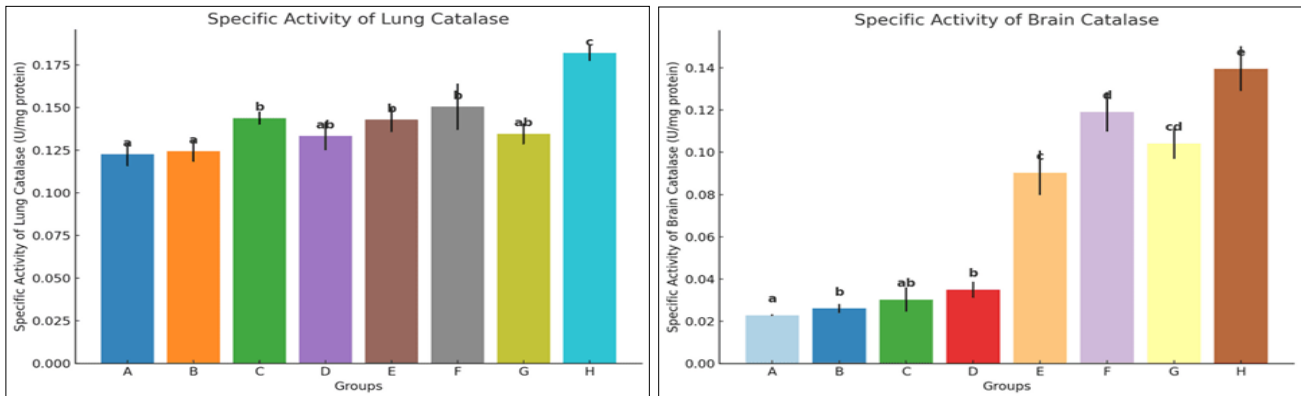


**Fig 2:** Specific Activity of Lung and Brain Catalase (CAT) in Rats Exposed to Dichlorvos, Dimethoate, and Cypermethrin Singly and in Combination. Plotted values are means  $\pm$  SEM. Bars carrying different alphabetical notations are significantly different ( $p \leq 0.05$ )

As illustrated in Figure 3a, lung malondialdehyde (MDA) concentrations differed significantly across the treatment groups ( $p < 0.05$ ). The control group (Group A) exhibited the lowest MDA levels and did not differ significantly from Group B ( $p > 0.05$ ). A modest but significant increase was observed in Group C relative to Groups A and B ( $p < 0.05$ ). Group D showed a further elevation, with values overlapping statistically with those of Groups C and E, indicating comparable degrees of oxidative injury. Although Group E remained significantly higher than Groups A–C ( $p < 0.05$ ), its MDA concentration was slightly lower than those observed in Groups F and G. Groups F and G displayed comparable MDA levels ( $p > 0.05$ ), both of which were significantly higher than those of the earlier treatment groups. The highest lung MDA concentration was recorded in Group H, which differed significantly from all other groups ( $p < 0.05$ ). Overall, these findings demonstrate a progressive increase in lipid peroxidation in the lungs, with the most severe oxidative damage occurring in the triple-insecticide exposure group.

Figure 3b depicts the pattern of brain MDA concentrations, which showed a somewhat different trend. Groups A and B recorded similarly low MDA levels, with no significant difference between them ( $p > 0.05$ ). Significant elevations were evident in Groups C and D compared with Groups A and B ( $p < 0.05$ ), although the two groups did not differ significantly from each other, indicating comparable induction of oxidative stress. Group E exhibited a reduction relative to Groups C and D; however, its MDA level remained significantly higher than those of Groups A and B ( $p < 0.05$ ). A further significant increase was observed in Group F compared with Group E ( $p < 0.05$ ), reflecting heightened lipid peroxidation, whereas Group G showed a decrease to levels statistically comparable with Group E ( $p > 0.05$ ). Group H again displayed the highest MDA concentration, which was significantly greater than all other groups ( $p < 0.05$ ).

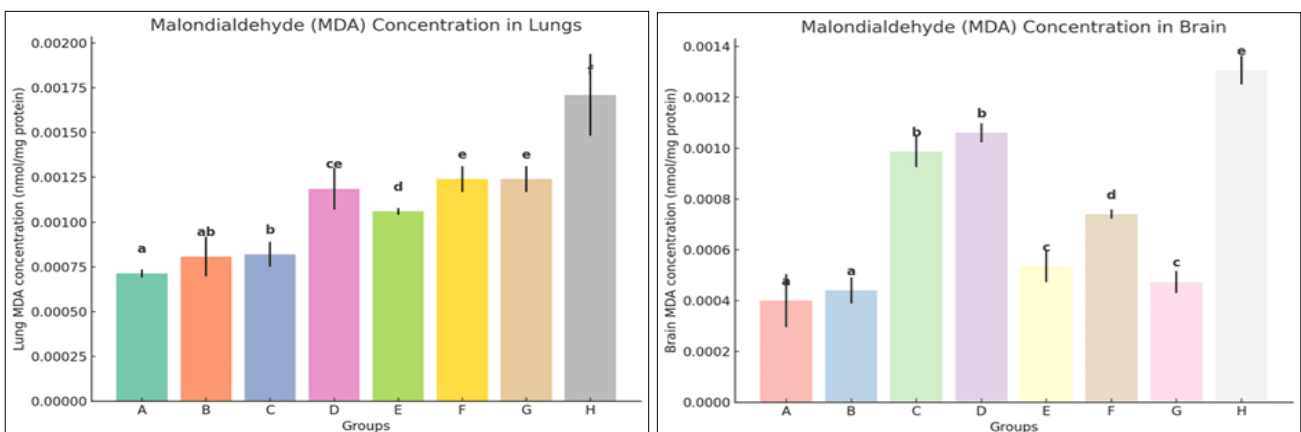


**Fig 3:** Concentration of Lung and Brain Malondialdehyde (MDA) in Rats Exposed to Dichlorvos, Dimethoate, and Cypermethrin Singly and in Combination. Plotted values are means  $\pm$  SEM. Bars carrying different alphabetical notations are significantly different ( $p \leq 0.05$ )

The histopathological evaluation of brain and lung tissues from postpartum female Wistar albino rats exposed to dichlorvos, dimethoate, cypermethrin, and their combinations revealed exposure-dependent structural alterations, with severity varying according to the type and combination of insecticides administered.

**Brain Histopathology (Plates 1 A–H):**

Plate 1A (Group A) representing the control group showed normal cortical architecture with well-organised neuronal layers. The multiform layer contained small pleomorphic cells, the granular layer was densely populated with intact granular cells, and the pyramidal layer exhibited large, well-defined pyramidal neurons embedded within a normal axonal fibre network. No degenerative or vascular abnormalities were observed.

In Plate 1B (Group B), dichlorvos exposure resulted in mild to moderate neuropathological changes, characterised by degeneration of the pyramidal layer and evident nuclear pyknosis in polymorphic cells of the multiform layer. These findings indicate early neuronal injury compared to the control.

Plate 1C (Group C) revealed more severe alterations following dimethoate exposure, including prominent neuronal nuclear pyknosis, marked cerebral vascular stenosis, and axonal clumping. These changes reflect significant neuronal degeneration and vascular compromise.

In Plate 1D (Group D), cypermethrin exposure produced axonal degeneration, vascular endothelial separation, and

nuclear pyknosis of pyramidal cells, indicating concurrent neuronal and vascular damage.

Plate 1E (Group E), representing combined dichlorvos and dimethoate exposure, showed exacerbated neurodegeneration, with granular cell nuclear pyknosis and glial cell degeneration within the polymorphic layer, suggesting widespread cellular injury involving both neurons and supporting glial cells.

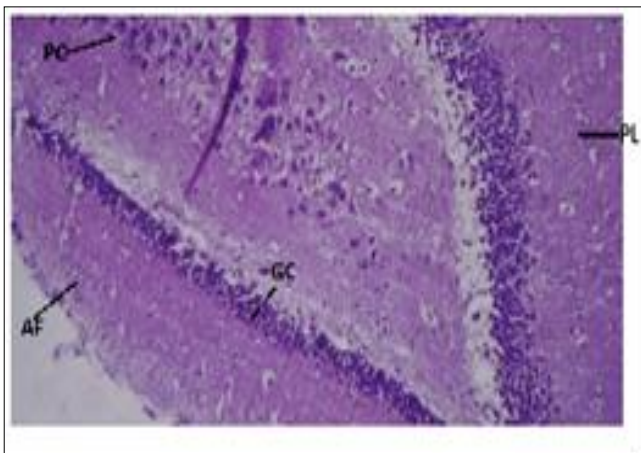
Plate 1F (Group F) demonstrated pronounced polymorphic layer cellular degeneration following combined dichlorvos and cypermethrin exposure, indicating advanced cortical injury compared to single-exposure groups.

In contrast, Plate 1G (Group G), representing combined dimethoate and cypermethrin exposure, showed largely preserved cortical organisation. Pleomorphic, pyramidal, and granular cell layers appeared normal, with no overt signs of degeneration.

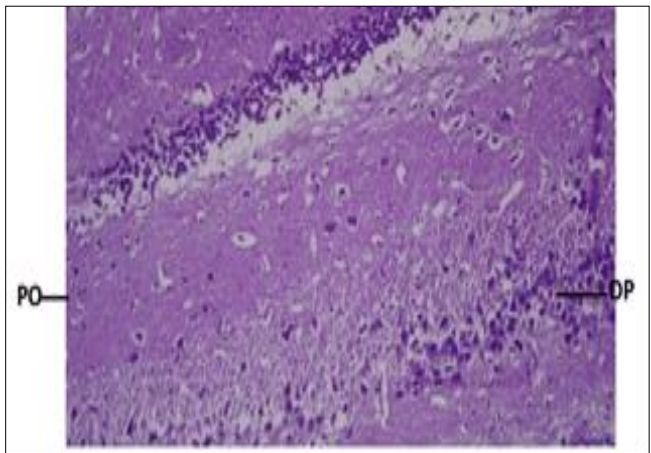
Plate 1H (Group H) exhibited the most severe neuropathological changes. Extensive neuronal cell clumping and widespread nuclear pyknosis were observed, indicating profound neurodegeneration and disruption of normal cortical architecture following triple-insecticide exposure.

**Notation**

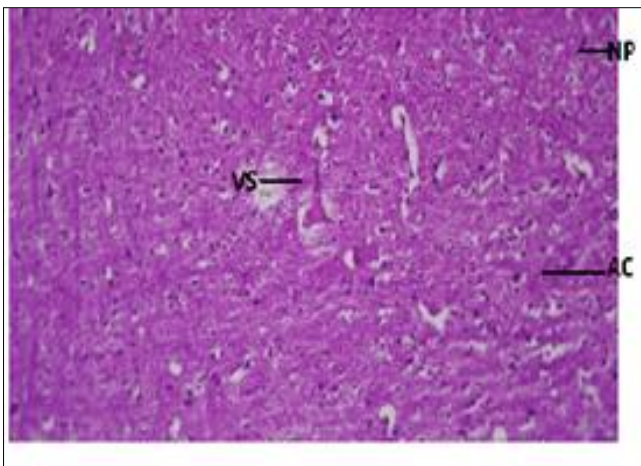
PC – pyramidal cell; GC – granular cell; PL – polymorphic layer; AF – axonal fibres; NP – nuclear pyknosis; AD – axonal degeneration; VS – vascular stenosis; AC – axonal clumping; GD – glial degeneration; NC – neuronal clumping.



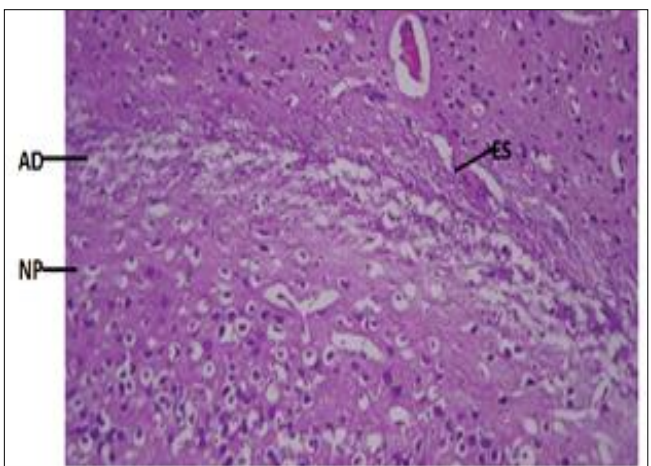
A



B



C



D

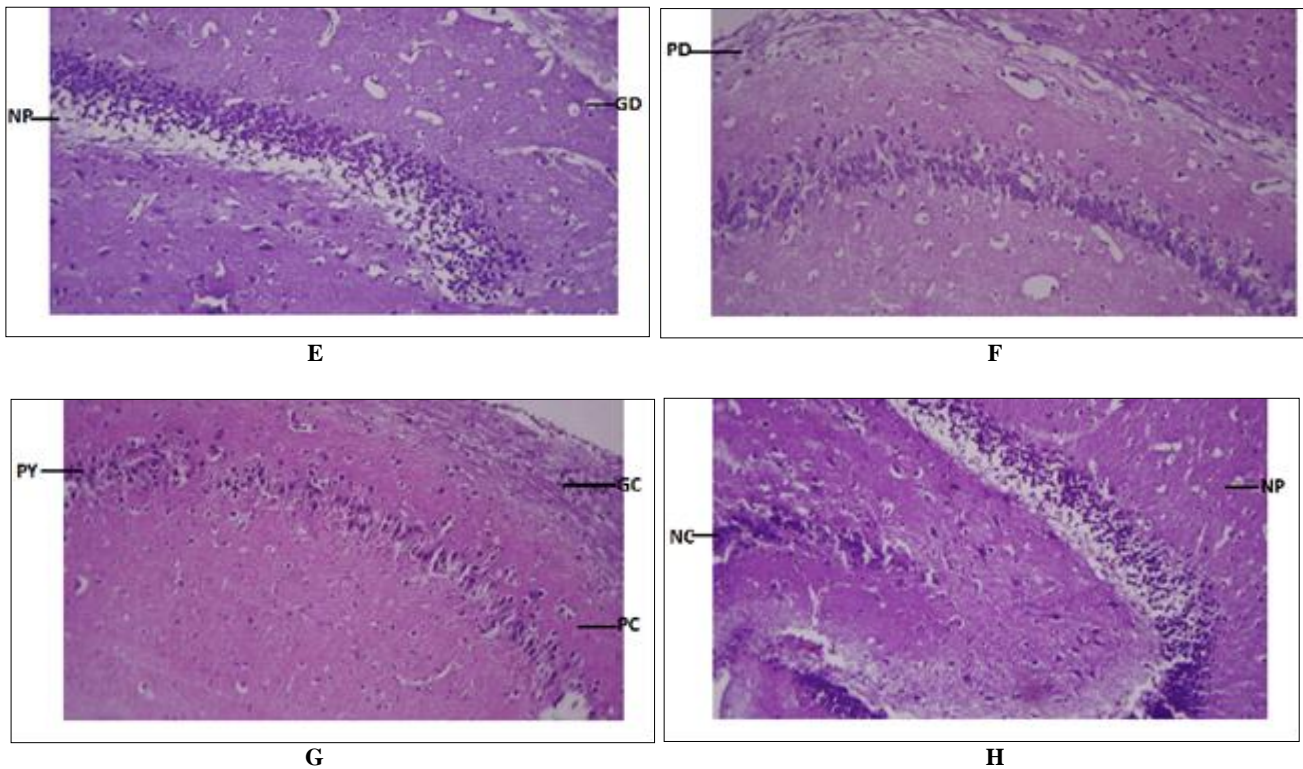


**Plate 1 (A–H):** Histopathological photomicrographs of the brain of postpartum female Wistar albino rats showing representative cortical alterations following exposure to single and combined insecticides (H&E, ×100).

**Lung Histopathology (Plates 2 A–H)**

Plate 2A (Group A) showed normal pulmonary histology, with patent alveolar spaces, intact terminal bronchioles, normal interstitial spaces, and well-preserved bronchial arteries, confirming baseline lung integrity.

In Plate 2B (Group B), dichlorvos exposure induced alveolar collapse, bronchiolar luminal secretions, and the presence of follicular anthracophages, indicating early inflammatory and structural lung injury.

Plate 2C (Group C) revealed severe pulmonary pathology following dimethoate exposure, characterised by marked interstitial haemorrhage, extensive vascular degeneration, and dense inflammatory exudates within the lung parenchyma.

In Plate 2D (Group D), cypermethrin exposure resulted in severe bronchiolar necrosis, areas of atelectasis, and vascular degeneration, indicating significant airway and alveolar compromise.

Plate 2E (Group E), representing combined dichlorvos and dimethoate exposure, showed relatively preserved lung architecture, with normal alveolar spaces, intact terminal bronchioles, and preserved bronchial arteries, with minimal observable pathology.

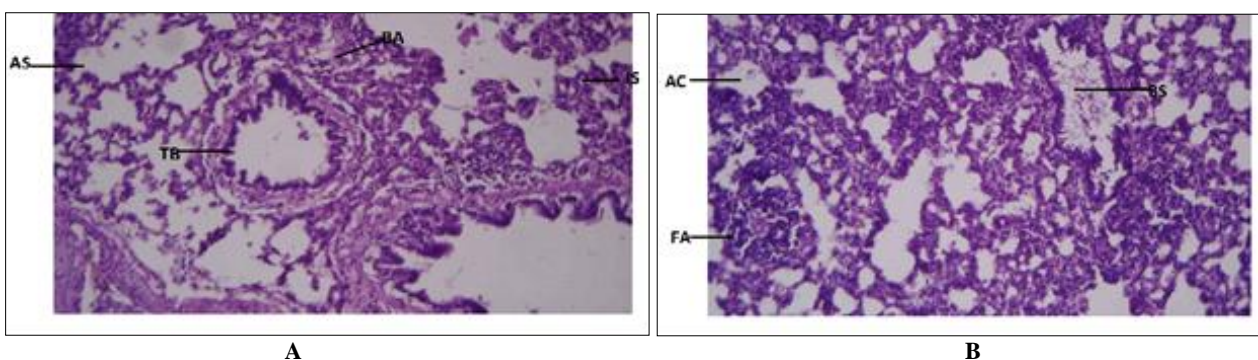
Plate 2F (Group F) demonstrated mixed pulmonary alterations following combined dichlorvos and cypermethrin exposure. While alveolar architecture remained largely normal, focal bronchiolar ulceration and inflammatory exudates were evident.

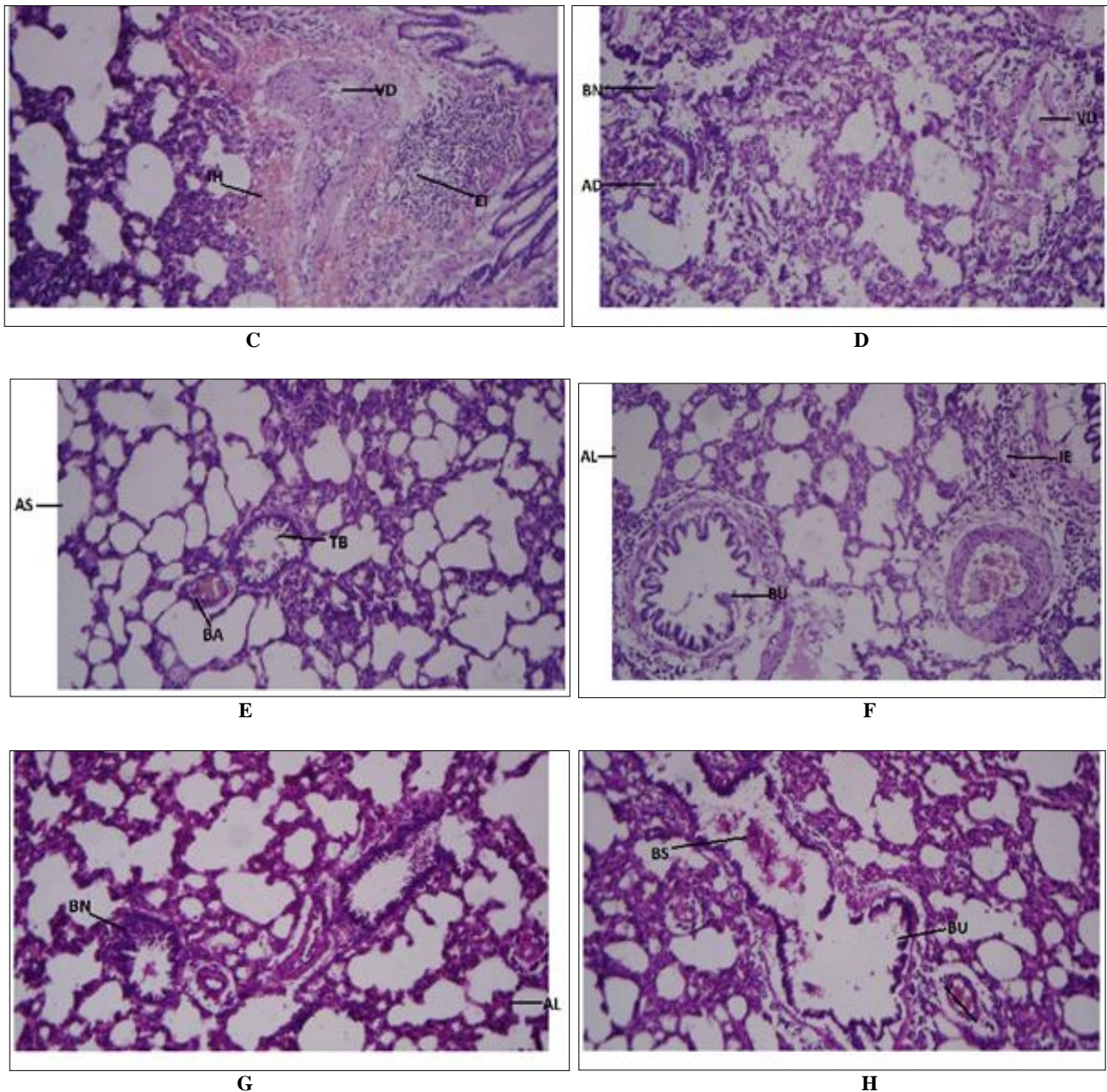
Plate 2G (Group G) showed predominantly normal alveolar structures with focal bronchiolar necrosis in rats exposed to dimethoate and cypermethrin, suggesting selective airway involvement.

Plate 2H (Group H) revealed pronounced pulmonary damage in the triple-insecticide group, characterised by bronchiolar ulceration and luminal secretions, indicating severe airway injury and inflammatory response.

**Notations**

AS – Alveolar spaces, TB – Terminal bronchiole, IS – Interstitial space, BA – Bronchial artery, AC – Alveolar collapse(s), BS – Bronchiolar secretions, FA – Follicular anthracophages, IH – Interstitial haemorrhage, VD – Vascular degeneration, EI – Exudates of inflammation, BN – Bronchiolar necrosis, AD – Atelectasis, AL – Alveoli (normal alveoli), BU – Bronchiolar ulceration, IE – Inflammatory exudates





**Plate 2 (A–H):** Histopathological photomicrographs of the lung of postpartum female Wistar albino rats showing representative cortical alterations following exposure to single and combined insecticides (H&E,  $\times 100$ ).

Across Plates 1–2, histopathological findings demonstrate that both brain and lung tissues were adversely affected by insecticide exposure, with the severity of lesions increasing under combined treatments. Single-insecticide exposures produced variable neuronal and pulmonary damage, whereas combined exposures—particularly the triple-insecticide treatment—resulted in the most extensive structural disruption. These results indicate organ-specific and mixture-dependent toxic effects, with the brain and lungs exhibiting heightened vulnerability to combined insecticide exposure.

### Discussion

The antioxidant enzyme response patterns observed in this study provide a clear biochemical framework for understanding the organ-specific oxidative stress induced by single and combined insecticide exposures. The progressive increase in superoxide dismutase (SOD) activity observed in the lungs (Figure 1a) reflects an adaptive cellular response

to elevated production of superoxide radicals following insecticide exposure. The lack of significant difference between the control and lowest exposure groups indicates that basal antioxidant defences were sufficient to neutralise reactive oxygen species at minimal exposure levels. However, the stepwise elevation in SOD activity across higher treatment groups suggests increasing oxidative pressure on pulmonary tissues (Rogers & Cismowski, 2017)<sup>[39]</sup>. The marked induction in the triple-insecticide group underscores the synergistic nature of combined exposures, where multiple toxicants appear to overwhelm normal detoxification pathways, necessitating enhanced enzymatic defence. Given the lungs' role as a primary interface for inhaled toxicants, this response highlights their vulnerability to oxidative insult and the cumulative impact of pesticide mixtures (Benka-Coker *et al.*, 2020)<sup>[5]</sup>.

A similar but more pronounced trend was evident in brain SOD activity (Figure 1b), suggesting heightened sensitivity of neural tissue to oxidative challenges. The sharper

distinctions between treatment groups indicate that neuronal cells may respond more rapidly and intensely to rising oxidative stress. This heightened response may be attributed to the brain's high metabolic demand, elevated oxygen utilisation, and abundance of oxidisable lipid substrates (Franzoni *et al.*, 2021)<sup>[13]</sup>. The substantial increase in SOD activity in the higher exposure groups, particularly under combined treatments, suggests that reactive oxygen species generation in neural tissue exceeded baseline antioxidant capacity, prompting a robust compensatory response (Imam *et al.*, 2024; Karataş & Çakır, 2024)<sup>[19, 23]</sup>.

Catalase activity further corroborated the involvement of oxidative stress mechanisms in both organs. The lung catalase response (Figure 2a) exhibited a gradual but consistent increase across exposure groups, reflecting enhanced decomposition of hydrogen peroxide generated downstream of SOD activity. The intermediate positioning of several treatment groups suggests a balanced but strained antioxidant response, while the pronounced elevation in the triple-combination group indicates substantial hydrogen peroxide burden. This pattern reinforces the concept that combined insecticide exposure amplifies oxidative challenges beyond those induced by individual compounds (Alves *et al.*, 2024)<sup>[2]</sup>.

In contrast, brain catalase activity (Figure 2b) displayed a more stratified pattern, with clearer separation between low and high exposure groups. The sharp rise in catalase activity at higher treatment levels implies a critical threshold beyond which neural tissues experience excessive hydrogen peroxide accumulation (Ferrazza *et al.*, 2023; Saka *et al.*, 2023)<sup>[12, 40]</sup>. The brain's comparatively limited antioxidant reserve may account for this pronounced response, as neuronal cells rely heavily on tightly regulated redox balance to maintain functional integrity. The distinct escalation in catalase activity in the combined exposure groups suggests that the brain is particularly susceptible to oxidative perturbations arising from pesticide mixtures (Constantinescu *et al.*, 2025; Lorke & Öz, 2025)<sup>[7, 8, 27]</sup>.

Lipid peroxidation, assessed via malondialdehyde (MDA) concentrations, provided direct evidence of oxidative damage to cellular membranes. The progressive increase in lung MDA levels (Figure 3a) closely mirrored the trends observed for antioxidant enzymes, indicating that despite enzymatic upregulation, oxidative injury still occurred. The overlap among intermediate groups suggests partial containment of oxidative damage, whereas the substantial elevation in the triple-insecticide group reflects a breakdown of protective mechanisms. This pattern underscores the inability of antioxidant defences to fully counteract lipid oxidation under combined toxicant exposure (Gopikrishnan *et al.*, 2024; Kamalakannan *et al.*, 2024)<sup>[16, 22]</sup>.

Brain MDA levels (Figure 3b) exhibited greater variability across treatment groups, highlighting complex dynamics between oxidative insult and antioxidant compensation in neural tissue. The fluctuations observed in intermediate groups may reflect transient adaptive responses or differential activation of repair mechanisms. However, the pronounced elevation in the triple-combination group clearly indicates cumulative lipid peroxidation and structural membrane damage. This finding is particularly concerning given the central role of membrane integrity in neuronal signalling and synaptic function (Jové *et al.*, 2023; Rao *et al.*, 2024)<sup>[21, 37]</sup>.

The histopathological findings from Plates 1–2 provide clear morphological evidence of tissue-specific and mixture-

dependent toxicity following exposure to dichlorvos, dimethoate, cypermethrin, and their combinations. The progressive structural alterations observed in both brain and lung tissues align with the biochemical indicators of oxidative stress reported earlier, reinforcing oxidative injury as a central mechanism underlying the observed pathology.

In the brain (Plates 1 A-H), the control group displayed intact cortical organisation with clearly defined neuronal layers and preserved axonal networks, reflecting normal neuroanatomical integrity. This baseline architecture underscores that the observed lesions in exposed groups were treatment-induced rather than artefactual. Single-insecticide exposure resulted in distinct yet overlapping neuropathological features. Dichlorvos exposure produced early degenerative changes, particularly within the pyramidal layer, accompanied by nuclear pyknosis in polymorphic cells. These findings suggest selective neuronal vulnerability and early chromatin condensation, indicative of metabolic stress and impaired cellular viability (Mateo *et al.*, 2022; Orekhova *et al.*, 2021)<sup>[30, 35]</sup>.

Dimethoate exposure elicited more severe neuropathology, characterised by extensive neuronal nuclear pyknosis, axonal clumping, and marked vascular stenosis. The vascular involvement implies compromised cerebral perfusion, which may exacerbate neuronal injury by limiting oxygen and nutrient delivery. Axonal clumping further suggests disruption of neuronal connectivity and impaired signal transmission, pointing to functional as well as structural deficits. Cypermethrin exposure similarly induced axonal degeneration and pyramidal cell nuclear pyknosis, accompanied by vascular endothelial separation. The concurrent neuronal and vascular damage observed in this group highlights the capacity of cypermethrin to destabilise both neural cells and the neurovascular unit (Imam *et al.*, 2024)<sup>[19]</sup>.

Combined exposures produced variable but generally more severe outcomes. The dichlorvos–dimethoate combination resulted in pronounced neuronal and glial degeneration, indicating that dual exposure intensified cellular injury beyond that seen with individual compounds. The involvement of glial cells is particularly significant, as glial dysfunction compromises neuronal support, antioxidant buffering, and homeostatic regulation, thereby amplifying neurodegenerative processes (Constantinescu *et al.*, 2025)<sup>[7, 8]</sup>. The dichlorvos–cypermethrin combination produced extensive polymorphic layer degeneration, suggesting synergistic toxicity and widespread cortical involvement (Petrovici *et al.*, 2025)<sup>[36]</sup>. In contrast, the dimethoate–cypermethrin combination showed relatively preserved cortical architecture, indicating that not all pesticide combinations exert equivalent neurotoxic interactions. This observation underscores the complexity of mixture toxicology and suggests that chemical interactions may be additive, synergistic, or partially antagonistic depending on the compounds involved (Petrovici *et al.*, 2025)<sup>[36]</sup>. The observed ischemic changes and pyknotic nuclei in neuronal tissues, especially in hippocampal layers and the cerebral cortex, are consistent with previous reports on cypermethrin-induced neurotoxicity (Sayım *et al.*, 2005)<sup>[41]</sup>. The most severe neuropathological alterations were observed in the triple-insecticide group, where widespread neuronal clumping and nuclear pyknosis reflected advanced neurodegeneration and loss of cortical organisation. These lesions signify extensive cellular injury and breakdown of

normal neuronal architecture, consistent with overwhelming oxidative stress and failure of compensatory defence mechanisms (Igben *et al.*, 2023) <sup>[18]</sup>. The severity of these changes supports the notion that combined exposure to multiple insecticides poses a substantially greater neurotoxic risk than single or dual exposures.

Pulmonary histopathology (Plates 2 A–H) similarly demonstrated a spectrum of injury that progressed with exposure complexity. The control lungs exhibited normal alveolar architecture, patent air spaces, intact bronchioles, and preserved vascular structures, confirming healthy pulmonary function. Dichlorvos exposure resulted in alveolar collapse, bronchiolar secretions, and the presence of anthracophages, reflecting early inflammatory responses and impaired alveolar stability. These changes suggest disruption of normal ventilation and initiation of pulmonary defence mechanisms (Abdo *et al.*, 2021) <sup>[1]</sup>.

Dimethoate exposure produced the most severe lung pathology among single-insecticide groups, characterised by extensive interstitial haemorrhage, vascular degeneration, and dense inflammatory exudates. Such lesions indicate profound damage to the alveolar–capillary barrier, with serious implications for gas exchange and pulmonary perfusion. Cypermethrin exposure also caused severe pulmonary injury, including bronchiolar necrosis, atelectasis, and vascular degeneration, highlighting significant airway destruction and alveolar collapse (Morsi *et al.*, 2023; SEVEN *et al.*, 2022) <sup>[32, 43]</sup>.

Combined exposures again demonstrated differential effects. The dichlorvos–dimethoate group showed relatively preserved lung architecture, suggesting a degree of compensatory adaptation or reduced pulmonary synergy at the administered doses. In contrast, the dichlorvos–cypermethrin and dimethoate–cypermethrin combinations produced focal bronchiolar ulceration and necrosis, respectively, indicating selective vulnerability of airway epithelium despite relatively intact alveolar structures. These findings imply that combined exposures may target specific pulmonary compartments rather than producing uniform damage (Takeuchi *et al.*, 2021) <sup>[47]</sup>.

The most pronounced pulmonary lesions were observed in the triple-insecticide group, where bronchiolar ulceration and luminal secretions reflected severe airway injury, epithelial erosion, and sustained inflammatory responses. Such pathology would be expected to compromise airway patency, mucociliary clearance, and overall respiratory efficiency. The convergence of airway ulceration and excessive secretions highlights the cumulative and synergistic nature of pulmonary toxicity under combined insecticide exposure (Lopes-Ferreira *et al.*, 2023; Petrovici *et al.*, 2025) <sup>[26, 36]</sup>.

## Conclusion

Overall, the integrated evaluation of biochemical and histopathological findings demonstrates a clear and coherent relationship between insecticide exposure, antioxidant enzyme modulation, lipid peroxidation, and tissue injury in both lung and brain tissues. Both organs exhibited marked evidence of oxidative stress; however, the brain showed sharper gradations in enzymatic responses and more variable lipid peroxidation patterns, indicating heightened vulnerability and a comparatively limited adaptive capacity. The consistently greater biochemical disturbances and structural damage observed under combined insecticide

exposures, particularly the triple-insecticide treatment, underscore the synergistic toxicity of pesticide mixtures and reveal the limitations of assessing single compounds in isolation. Histopathological evidence further confirms that the brain and lungs are major target organs of insecticide toxicity, with combined exposures producing the most extensive neuronal degeneration, vascular compromise, inflammatory infiltration, and architectural disruption. The strong concordance between oxidative stress biomarkers and tissue pathology highlights redox imbalance as a unifying mechanism of toxicity. Collectively, these findings emphasise the elevated health risks associated with pesticide mixtures and reinforce the necessity for toxicological evaluations that incorporate organ-specific responses and mixture effects to more accurately reflect real-world exposure scenarios.

## References

1. Abdo W, Elmadawy MA, Abdelhiee EY, Abdel-Kareem MA, Farag AES, Aboubakr M, *et al.* Protective effect of thymoquinone against lung intoxication induced by malathion inhalation. *Scientific Reports*, 2021, 11(1). <https://doi.org/10.1038/s41598-021-82083-w>
2. Alves T, Trivellato MF, Freitas TAL, Kato AY, Gomes CRA, Ferraz YMM, *et al.* Pollen contaminated with a triple-action fungicide induced oxidative stress and reduced bee longevity though with less impact on lifespan in bees from well fed colonies. *Research Square*, 2024. <https://doi.org/10.21203/rs.3.rs-4836495/v1>
3. Anwar S, Alrumaihi F, Sarwar T, Babiker AY, Khan AA, Prabhu SV, *et al.* Exploring therapeutic potential of catalase: strategies in disease prevention and management. *Biomolecules*, 2024, 14(6). <https://doi.org/10.3390/biom14060697>
4. Banerjee P, Gaddam N, Chandler V, Chakraborty S. Oxidative stress–induced liver damage and remodeling of the liver vasculature. *American Journal of Pathology*, 2023;193(10):1400–1412. <https://doi.org/10.1016/j.ajpath.2023.06.002>
5. Benka-Coker W, Hoskovec L, Severson R, Balmes JR, Wilson A, Magzamen S, *et al.* The joint effect of ambient air pollution and agricultural pesticide exposures on lung function among children with asthma. *Environmental Research*, 2020;190:109903. <https://doi.org/10.1016/j.envres.2020.109903>
6. Bezerra FS, Lanzetti M, Nesi RT, Nagato AC, Silva CPe, Kennedy-Feitosa E, *et al.* Oxidative stress and inflammation in acute and chronic lung injuries. *Antioxidants*, 2023;12(3):548. <https://doi.org/10.3390/antiox12030548>
7. Constantinescu AM, Karzi V, Docea AO, Tsitsimpikou C, Nosyrev AE, Tsatsakis A, *et al.* Neurobehavioral effects of low dose exposure to chemical mixtures: a review. *Archives of Toxicology*, 2025. <https://doi.org/10.1007/s00204-025-04009-z>
8. Constantinescu AM, Karzi V, Docea AO, Tsitsimpikou C, Nosyrev AE, Tsatsakis A, *et al.* Neurobehavioral effects of low dose exposure to chemical mixtures: a review. *Archives of Toxicology*, 2025;99(4):1315–1336. <https://doi.org/10.1007/s00204-025-04009-z>
9. Craig P, Dujardin B, Hart A, Hernández AF, Bennekou SH, Kneuer C, *et al.* Cumulative dietary risk

- characterisation of pesticides that have acute effects on the nervous system. *EFSA Journal*, 2020, 18(4). <https://doi.org/10.2903/j.efsa.2020.6087>
10. Elmorsy E, Al-Ghafari AB, Doghaither HAA, Salama M, Carter WG. An investigation of the neurotoxic effects of malathion, chlorpyrifos, and paraquat to different brain regions. *Brain Sciences*, 2022;12(8):975. <https://doi.org/10.3390/brainsci12080975>
  11. Farkhondeh T, Mehrpour O, Forouzanfar F, Roshanravan B, Samarghandian S. Oxidative stress and mitochondrial dysfunction in organophosphate pesticide-induced neurotoxicity and its amelioration: a review. *Environmental Science and Pollution Research*, 2020;27(20):24799–24814. <https://doi.org/10.1007/s11356-020-09045-z>
  12. Ferrazza MSHH, Magro DDD, Salamaia EM, Guareschi TE, Erzinger LFF, Maia TP, *et al.* Sub chronic administration of lead alters markers of oxidative stress, acetylcholinesterase and Na<sup>+</sup>K<sup>+</sup> ATPase activities in rat brain. *Acta Neurobiologiae Experimentalis*, 2023;83(2):216–228. <https://doi.org/10.55782/ane-2023-019>
  13. Franzoni F, Scarfò G, Guidotti S, Fusi J, Asomov MI, Pruneti C, *et al.* Oxidative stress and cognitive decline: the neuroprotective role of natural antioxidants. *Frontiers in Neuroscience*, 2021, 15. <https://doi.org/10.3389/fnins.2021.729757>
  14. Gaschler MM, Stockwell BR. Lipid peroxidation in cell death. *Biochemical and Biophysical Research Communications*, 2017;482(3):419–425. <https://doi.org/10.1016/j.bbrc.2016.10.086>
  15. Ghebryal LN, Noshay MM, El-Ghor AA, Eissa SM. Comparative analysis of *Acomys cahirinus* and *Mus musculus* responses to genotoxicity, oxidative stress, and inflammation. *Scientific Reports*, 2023, 13(1). <https://doi.org/10.1038/s41598-023-31143-4>
  16. Gopikrishnan M, Subramanian K, Krn A, Doss CGP, Srimuruganandam B, Chandrasekaran N, *et al.* Particulate matter and nanoplastics: synergistic impact on *Artemia salina*. *Environmental Science Atmospheres*, 2024;4(9):988–999. <https://doi.org/10.1039/d4ea00065j>
  17. He J, Zhang K, Wang L, Du Y, Yang Y, Yuan C, *et al.* Highly efficient degradation of cypermethrin by a co-culture of *Rhodococcus* sp. JQ-L and *Comamonas* sp. A-3. *Frontiers in Microbiology*, 2022, 13. <https://doi.org/10.3389/fmicb.2022.1003820>
  18. Igben VO, Iju WJ, Itivere OA, Oyem JC, Akpulu P, Ahama EE, *et al.* *Datura metel* stramonium exacerbates behavioral deficits, medial prefrontal cortex, and hippocampal neurotoxicity in mice via redox imbalance. *Laboratory Animal Research*, 2023, 39(1). <https://doi.org/10.1186/s42826-023-00162-7>
  19. Imam AL, Okesina AA, Sulamon FA, Imam A, Ibiyeye RY, Oyewole LA, *et al.* Orally administered thymoquinone mitigates cypermethrin-induced dentate gyrus oxidative stress, preventing GABAergic interneuron degeneration and memory impairment in rats via the Nrf2/ARE pathway. *Research Square*, 2024. <https://doi.org/10.21203/rs.3.rs-4130260/v1>
  20. Jomová K, Raptová R, Alomar SY, Alwasel S, Nepovimová E, Kuča K, *et al.* Reactive oxygen species, toxicity, oxidative stress, and antioxidants: chronic diseases and aging. *Archives of Toxicology*, 2023;97(10):2499–2525. <https://doi.org/10.1007/s00204-023-03562-9>
  21. Jové M, Mota-Martorell N, Òbis È, Sol J, Martin-Garí M, Ferrer I, *et al.* Lipid adaptations against oxidative challenge in the healthy adult human brain. *Antioxidants*, 2023;12(1):177. <https://doi.org/10.3390/antiox12010177>
  22. Kamalakannan M, Rajendran D, Thomas J, Chandrasekaran N. Synergistic impact of nanoplastics and nanopesticides on *Artemia salina* and toxicity analysis. *Nanoscale Advances*, 2024;6(12):3119–3131. <https://doi.org/10.1039/d4na00013g>
  23. Karataş T, Çakır M. Assessment of deltamethrin-induced DNA damage, neurotoxic and neuroimmune effects in the brain tissue of brown trout (*Salmo trutta fario*). *Veterinárni Medicína*, 2024;69(3):77–89. <https://doi.org/10.17221/115/2023-vetmed>
  24. Kong J, Fan R, Zhang Y, Jia Z, Zhang J, Pan H, *et al.* Oxidative stress in the brain–lung crosstalk: cellular and molecular perspectives. *Frontiers in Aging Neuroscience*, 2024;16:1389454. <https://doi.org/10.3389/fnagi.2024.1389454>
  25. Langenbach T, Campos TMPde, Caldas LQA. Why airborne pesticides are so dangerous. *IntechOpen*, 2021. <https://doi.org/10.5772/intechopen.95581>
  26. Lopes-Ferreira M, Farinha LRL, Costa YSO, Pinto FJ, Disner GR, Rosa JGS, *et al.* Pesticide-induced inflammation at a glance. *Toxics*, 2023;11(11):896. <https://doi.org/10.3390/toxics11110896>
  27. Lorke DE, Öz M. A review on oxidative stress in organophosphate-induced neurotoxicity. *The International Journal of Biochemistry and Cell Biology*, 2025;180:106735. <https://doi.org/10.1016/j.biocel.2025.106735>
  28. Mackei M, Huber FX, Oláh B, Neogrády Z, Mátis G. Redox metabolic disruptions in the honey bee brain following acute exposure to the pyrethroid deltamethrin. *Scientific Reports*, 2025;15(1):28322. <https://doi.org/10.1038/s41598-025-14089-7>
  29. Massoud A, SaadAllah MS, Dahan N, Nasr NE, El-Fkharany I, Ahmed MS, *et al.* Toxicological effects of malathion at low dose on Wister male rats with respect to biochemical and histopathological alterations. *Frontiers in Environmental Science*, 2022, 10. <https://doi.org/10.3389/fenvs.2022.860359>
  30. Mateo EM, Tonino RPB, Cantó A, Monroy-Noyola A, Miranda M, Soria JM, *et al.* The neurotoxic effect of ochratoxin-A on the hippocampal neurogenic niche of adult mouse brain. *Toxins*, 2022;14(9):624. <https://doi.org/10.3390/toxins14090624>
  31. Misra HP, Fridovich I. The role of superoxide anion in the autooxidation of epinephrine and a simple assay for superoxide dismutase. *Journal of Biological Chemistry*, 1972;247(10):3170–3175.
  32. Morsi AA, Faruk EM, Mogahed MM, Baioumy B, Hussein A, El-shafey RS, *et al.* Modeling the effects of cypermethrin toxicity on ovalbumin-induced allergic pneumonitis rats: macrophage phenotype differentiation and p38/STAT6 signaling are candidate targets of pirfenidone treatment. *Cells*, 2023;12(7):994. <https://doi.org/10.3390/cells12070994>
  33. Ohkawa H, Ohishi N, Yagi K. Assay for lipid peroxides in animal tissues by thiobarbituric acid reaction. *Analytical Biochemistry*, 1979;95(2):351–358. [https://doi.org/10.1016/0003-2697\(79\)90738-3](https://doi.org/10.1016/0003-2697(79)90738-3)
  34. Okonkwo CO, Uyang GA, Okonkwo SN. Assessing the biochemical implication of using *Stachytarpheta*

- cayennensis* essential oil as an alternative to synthetic pesticides in Calabar Nigeria. Research Square, 2023. <https://doi.org/10.21203/rs.3.rs-3664402/v1>
35. Orekhova K, Mazzariol S, Sussan B, Bucci MG, Bonsembiante F, Verin R, *et al.* Immunohistochemical markers of apoptotic and hypoxic damage facilitate evidence-based assessment in pups with neurological disorders. *Veterinary Sciences*,2021;8(10):203. <https://doi.org/10.3390/vetsci8100203>
  36. Petrovici A, Săvuță G, Lucini C, Robea MA, Solcan C. Combined neurotoxic effects of commercial formulations of pyrethroid (deltamethrin) and neonicotinoid (imidacloprid) pesticides on adult zebrafish (*Danio rerio*). *Life*,2025;15(4):538. <https://doi.org/10.3390/life15040538>
  37. Rao GN, Jupudi S, Devarakonda KP, Bharathi J, Baba MZ, Justin A, *et al.* Azilsartan and ceftriaxone, a novel combination ameliorates excitotoxicity mediated neuroinflammation in *in-vitro* and *in-vivo* models of cerebral is chemia. *Research Square*, 2024. <https://doi.org/10.21203/rs.3.rs-3933469/v1>
  38. Rodrigues JA, Narasimhamurthy RK, Joshi MB, Dsouza HS, Mumbreakar KD. Pesticides exposure-induced changes in brain metabolome: implications in the pathogenesis of neurodegenerative disorders. *Neurotoxicity Research*,2022;40(5):1539–1554. <https://doi.org/10.1007/s12640-022-00534-2>
  39. Rogers LK, Cismowski MJ. Oxidative stress in the lung – the essential paradox. *Current Opinion in Toxicology*,2017;7:37–43. <https://doi.org/10.1016/j.cotox.2017.09.001>
  40. Saka VP, Vellapandian C, Narayanasamy D. Protective role of hispolon pyrazole and hispolon monomethyl ether pyrazole in electromagnetic radiation-induced behavioral, neurochemical, oxidative, and histological changes in rats. *Journal of Herbmed Pharmacology*,2023;12(2):299–308. <https://doi.org/10.34172/jhp.2023.32>
  41. Sayım F, Yavaşoğlu NÜK, Uyanıkgil Y, Aktuğ H, Yavaşoğlu A, Turgut M, *et al.* Neurotoxic effects of cypermethrin in Wistar rats: a haematological, biochemical and histopathological study. *Journal of Health Science*,2005;51(3):300–307. <https://doi.org/10.1248/jhs.51.300>
  42. Serdar O, Yıldırım N, Yıldırım NC. Single and combined effects of dimethoate and malathion on oxidative stress biomarkers in the non-target freshwater mussel *Dreissena polymorpha*. *Oceanological and Hydrobiological Studies*,2023;52(3):333–343. <https://doi.org/10.26881/oahs-2023.3.07>
  43. Seven B, Kültiğin Çavuşoğlu Y, Yalçın E, Acar A. Investigation of cypermethrin toxicity in Swiss albino mice with physiological, genetic and biochemical approaches. *Scientific Reports*,2022;12(1):11439. <https://doi.org/10.1038/s41598-022-15800-8>
  44. Sevim Ç, Taghizadehghalehjoughi A, Kara M. Effects of chlorpyrifos-methyl, chlormequat, deltamethrin, glyphosate, pirimiphos-methyl, tebuconazole and their mixture on oxidative stress and toxicity in HUVEC cell line. *Istanbul University Journal of Pharmacy*, 2021. <https://dergipark.org.tr/tr/pub/iujp/issue/63480/881724>
  45. Shaikh NI, Rs S. Exposure to chlorpyrifos and cypermethrin alone or in combination induces developmental abnormalities and lung damage in animal models: a review. *Journal of Entomology and Zoology Studies*,2020;8(5):1923–1931. <https://doi.org/10.22271/j.ento.2020.v8.i5aa.7769>
  46. Sinha AK. Colorimetric assay of catalase. *Analytical Biochemistry*,1972;47(2):389–394. [https://doi.org/10.1016/0003-2697\(72\)90132-7](https://doi.org/10.1016/0003-2697(72)90132-7)
  47. Takeuchi K, Kuroda Y, Numano T, Kimura M, Hayashi S, Furukawa S, *et al.* Comparison of acute inhalation toxicity of sulfuric acid by the inhalation and intratracheal instillation methods. *Journal of Toxicologic Pathology*,2021;34(3):269–276. <https://doi.org/10.1293/tox.2020-0086>
  48. Witwicka A, López-Orsorio F, Arce A, Gill RJ, Wurm Y. Acute and chronic pesticide exposure trigger fundamentally different molecular responses in bumble bee brains. *BMC Biology*,2025;23(1):72. <https://doi.org/10.1186/s12915-025-02169-z>
  49. Yousef MI, Roychoudhury S, Jafaar K, Sláma P, Kesari KK, Kamel MA. Aluminum oxide and zinc oxide induced nanotoxicity in rat brain, heart, and lung. *Physiological Research*, 2022, 677. <https://doi.org/10.33549/physiolres.934831>